

# Unifying Gompertzian growth with the communicable disease spreading paradigm

Matz Andreas Haugen<sup>a,\*</sup>, Dorothea Gilbert<sup>b</sup>

<sup>a</sup>*Enerhauggata 1, 0651 Oslo, Norway*

<sup>b</sup>*University of Oslo, Oslo, Norway*

---

## Abstract

Recently, a number of studies have shown that cumulative mortality followed a Gompertz curve in the initial Coronavirus epidemic period, March-April 2020. We show that the Gompertz curve is incompatible with the traditional communicable disease spreading hypothesis, and propose a new theory which better explains the nature of the mortality characteristics based on an environmental stressor. Second, we show that for the Gompertz curve to emerge, the stressor has to act on everyone simultaneously, rejecting the possibility of a disease propagation stage. Third, we show that the population acts like a coherent organism under growth/depletion. Finally, we connect the Susceptible-Infected-Recovered (SIR) model with our new theory and show that the SIR model is compatible with Gompertzian growth only when all nodes in the transmission network communicate with infinite speed and interaction.

*Keywords:* Gompertz, Coherence, Covid, Coronavirus, Network Analysis, Stochastic

---

## 1. Introduction

Traditional communicable disease spreading theory assumes a pathogen which infects the population through a network of transmission. Following this line of reasoning it can be shown that in the early stages of an epidemic, growth follows

---

\*Corresponding author

*Email address:* `matzhaugen@gmail.com` (Matz Andreas Haugen)

an initial exponential growth under a constant ratio of the infection rate and recovery rate. After the initial period, a logistic-like growth curve emerges, for which analytic solutions have recently emerged [1, 2, 3, 4, 5]. However, instead of showing logistic-like growth, observed cumulative mortality exhibits almost perfect resemblance to Gompertzian growth [6] where the log-transformed cumulative mortality, or log-mortality for short, is exponentially *decreasing* in time,

$$\frac{d}{dt} \ln Y(t) = -\beta \ln \frac{Y(t)}{\tilde{Y}} + \nu, \quad (1)$$

with constants  $\tilde{Y}$ ,  $\beta$ , and  $\nu$ , and whose solution is given as

$$Y(t) = Y_\infty \left( \frac{Y_0}{Y_\infty} \right)^{e^{-\beta t}} \quad (2)$$

$Y_0 = Y(t=0)$ ,  $Y_\infty = Y(t \rightarrow \infty) = \tilde{Y} e^{\nu/\beta}$  (see Fig. 1 for a conceptual image). Rarely do macroscopic observations reliant on social networks behave so closely to a model [7].

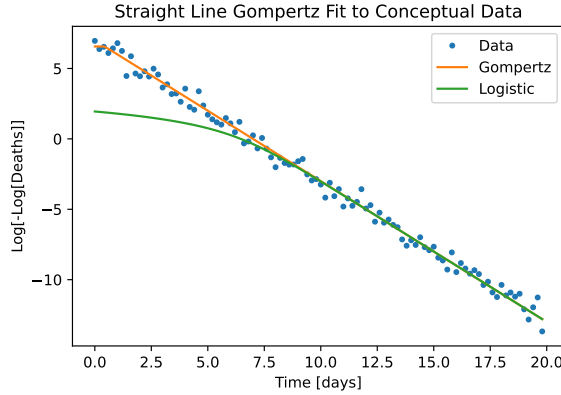


Figure 1: A conceptual display of the discrepancy seen between the logistic growth and the observations, superimposed by a Gompertz curve. Data is transformed to the straight line domain of the Gompertz curve for visual clarity,  $f(Y) = \ln \ln 1/Y$ .

5 This phenomenon is recorded by [8, 9, 10, 11, 12], showing Gompertz curves at national levels instead of the traditionally predicted logistic curves. What is

causing such a discrepancy between reality and the current theory of communicable diseases [13]?

One could approach this conundrum from parametrization of the Susceptible-Infected-Recovered (SIR) model under a time-dependent infection/recovery ratio,  $\phi(t)$ . How would  $\phi(t)$  have to behave? Start by recalling the SIR model for a pool of susceptible people of size  $N$  evolving between the three states susceptible,  $S(t)$ , recovered,  $R(t)$  and infected,  $I(t)$ ,

$$\frac{dS}{dt} = -\beta \frac{IS}{N} \quad (3)$$

$$\frac{dI}{dt} = -\beta \frac{IS}{N} - \alpha I. \quad (4)$$

$$\frac{dR}{dt} = \alpha I, \quad (5)$$

omitting the argument  $t$  in each variable for brevity and where  $\alpha$  and  $\beta$  in this  
10 context signify recovery and infection rates.

A line of reasoning employed by Rypdal and Rypdal [9] to obtain the Gompertz curve is to linearize the SIR model by assuming both the number of infected,  $I(t)$ , and cumulative infected,  $Y(t)$ , is much less than the total population,  $N \gg Y \geq I$ , which seems well founded at the national level,

$$\frac{dY}{dt} = \beta I \quad (6)$$

$$\frac{dI}{dt} = (\beta - \alpha)I = \alpha(\phi(t) - 1)I, \quad (7)$$

and where the number of recovered,  $R(t)$ , is under this linearization decoupled from the other variables.

They further assume the number of diseased is proportional to the number of cumulative infected, offset by a time lag, which allows us to use the same  
15 set of linearized equations to model the number of cumulative people diseased without loss of generality.

Due to this linearization, the infection/recovery ratio,  $\phi(t)$ , will have to change as a function of time to accommodate for the boundary conditions. And since  $I = I(Y)$ , we combine (6) via an instantaneous relative growth rate,  $\gamma(t) = dY(t)/(Y dt) = \beta I/Y$ , in turn parameterized by a scaling factor,  $\theta$ ,

representing the shape of the growth,

$$\frac{dY}{dt} = \gamma(t)Y(t) \quad (8a)$$

$$\gamma(t) = \frac{\gamma_\infty}{\theta} \left[ 1 - \left( \frac{Y}{Y_\infty} \right)^\theta \right], \quad (8b)$$

where  $\gamma_\infty = \gamma(t \rightarrow \infty)$ . This parametrization is the commonly used Richard's growth curve [14], also called  $\theta$ -logistic growth. Although not immediately justified in the communicable disease theory, one could imagine that  $\theta$  represents  
20 non-linear network behavior [15]. Note that at  $\theta = 1$ , the traditional logistic growth curve is obtained, while at  $\theta \rightarrow \infty$  we recover the exponential (Malthusian) explosion.

The observed Gompertzian mortality curves are realized in the limit  $\theta \rightarrow 0$ , with the relative growth rate,

$$\gamma(t) = \lim_{\theta \rightarrow 0} \frac{\gamma_\infty}{\theta} \left[ 1 - \left( \frac{Y}{Y_\infty} \right)^\theta \right] = \gamma_\infty \ln \frac{Y_\infty}{Y} \quad (9)$$

At this limit the growth rate approaches infinity as  $Y \rightarrow 0$ , which seems odd under the hypothesis that the pathogen has just started spreading. The Gompertzian limit also implies a decreasing relative growth rate from the very first  
25 time point, which under the SIR model seems unlikely given the large pool of susceptible people in the beginning. One would rather expect a near-constant relative growth rate in the early times. Rypdal and Rypdal [9] suggest that the decreasing relative growth rate is caused by social and political mitigating  
30 efforts, but these hardly justify such coherent and consistent mortality characteristics across countries. Perhaps a more likely scenario is the selective infection of central nodes in the transmission network resulting in an immediate decrease in relative growth. On the other hand, an infection of peripheral nodes should cause immediate exponential growth. Either case seems likely, and subject to  
35 initial conditions. Herrmann and Schwartz [16] studied a networked SIR model on a variety of networks, but did not elaborate on a possible fit to a Gompertz curve. Although it may be possible to realize Gompertzian growth from a special network, firm theoretical work has yet to be done to show this connection.

We will touch upon how the Gompertz curve emerges from one such network  
 40 below, under some caveats.

But even without the linearization and the somewhat arbitrary  $\theta$ -parametrization, one can still obtain growth which is almost Gompertzian, i.e. a straight line under a double-log transform of (2), viz.

$$\ln(\ln(Y_\infty/Y)) = -\beta t + k, \quad (10)$$

with  $k = \ln \ln \frac{Y_\infty}{Y_0}$ . To show this, we follow Carletti et al. [5] and consider the extended version of the SIR model by including a group of diseased,  $D(t)$ , such that  $N = S(t) + I(t) + R(t) + D(t)$ , also called the SIRD model. This requires an addition to our original set of ODEs (3), with a growth equation of the diseased group at some rate  $d$  relative to the current infected group,

$$\frac{dD}{dt} = \delta I. \quad (11)$$

Some algebraic manipulations reveal that the diseased group is described by a single ODE, viz.

$$\frac{dD}{dt} = \eta(1 - e^{-\xi D}) - \kappa D, \quad (12)$$

where  $\eta = \delta N$ ,  $\xi = \beta/(\delta N)$ ,  $\kappa = \delta + \alpha$ , and where  $N$  is assumed synonymous to the initial susceptible pool of people. This pool of people cannot be obtained from deaths alone, but can be inferred by assuming a known ratio between mortality and recovery,  $d$  and  $a$ . When only modeling the diseased however,  
 45 knowledge of  $N$  is irrelevant and the three parameters in (12) are sufficient.

Note here that at small values of  $D$  follow logistic growth,

$$\frac{dD}{dt} = bD(1 - D/K), \quad (13)$$

obtained with a second order expansion of the exponential term in 12 and with  $b = \eta\xi - \kappa$  and  $K = 2b/\eta\xi^2$ . The SIR model exhibits similar properties and its discrepancy with initial observations has been noted by others [17].

With the full 3-parameter single ODE of the diseased group in the SIRD  
 50 model, one can get almost arbitrarily close to the Gompertzian straight line in

the double-log domain even in the initial observations, although there will always be a non-zero concavity. Meanwhile, the Gompertz growth model can explain the initial observations with only two parameters, while the third parameter accounts for the discrepancy between the final observation,  $Y_{max}$ , and  $Y_{\infty}$ , an  
55 effect which is manifested as a tapering of the initial straight line in the double-log domain. These comparisons can be seen when fitting observations of diseased attributed to the Coronavirus in a variety of countries (Fig. 2 and Supplemental Information).

Note also that the macroscopic SIRD model does not consider network effects  
60 but assumes rather all entities to be connected and communicating at each time-step, usually justified through mean-field approximations [18]. It is however odd that observed mortality never exhibits a stage of near-exponential growth as this model predicts, but rather a constant slope in the double-log domain. We are thus prompted to look for another model which can explain the observations.

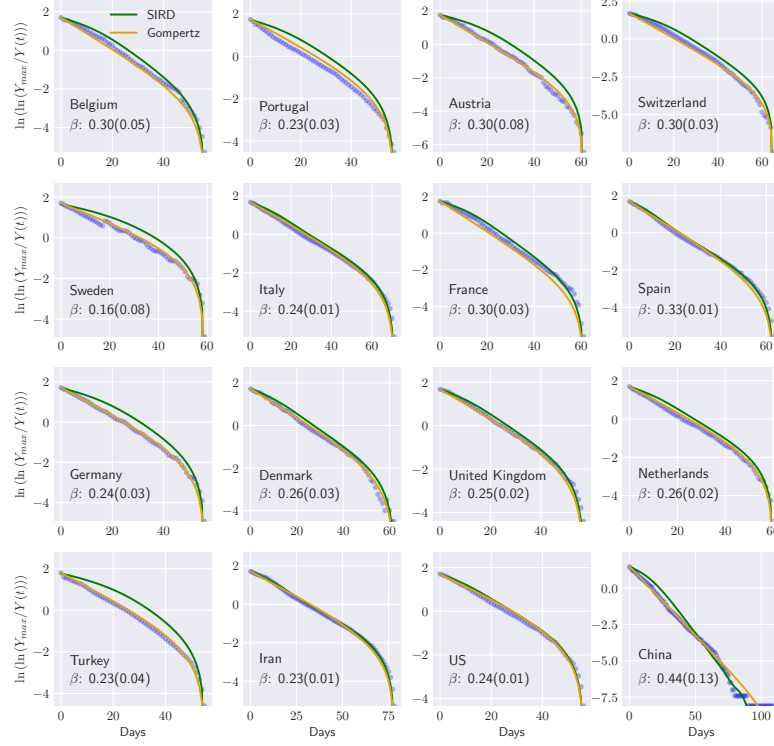


Figure 2: Cumulative diseased transformed by  $f(Y) = \ln \ln(Y_{max}/Y(t))$  plotted against number of days when  $Y(t)/Y_{max} > 0.005$ , comparing an SIRD with a Gompertz model. Both models are fit using non-linear least squares according to equations (1) and (12) in the text after normalizing, although the Gompertz curve can also be obtained with a simple linear fit using (10). The temporal evolution of the SIRD model is obtained from the Runge-Kutta algorithm. Each plot is annotated with an inferred transmission rate in the SIRD model, assuming bi-normally distributed parameter estimates. Fitting is done with Python-Scipy and a 6-day windowed average of deaths. Observations are taken from the Github repository compiled by the Center for Systems Science and Engineering (CSSE) at Johns Hopkins University, Baltimore, USA [19].

## 65 2. An alternative theory for observed mortality

An alternative line of reasoning that does not rely on the framework of communicable diseases is that the biosphere was perturbed by an external stressor, initiating a stress response to eventually bring mortality rates back to stability. This could explain the immediate dampening of mortality growth we see. Inspired by De Lauro et al. [20], the stressor can be modeled as a multiplicative stochastic dampening term at the microscopic level along with the countering force of the immune system. As with all multiplicative processes, it is convenient to log-transform normalized mortality with variables  $F(t) = Y(t)/Y_\infty$  and  $Z = \ln F$ , from which a natural perturbation model emerges,

$$dZ(t) = -\beta Z(t)dt + \sqrt{\sigma}dW(t), \quad (14)$$

where  $W(t)$  is a delta-correlated Wiener process<sup>1</sup>. Notice that this is just a continuous version of an AR(1) model. The diffusion coefficient,  $\sigma$ , represents the strength of the perturbation, which we directly see if we recast this equation in terms of mortality while introducing a new parameter  $K = \exp(-\frac{\sigma}{2\beta})$ , viz.

$$dF(t) = \left\{ \frac{\sigma}{2}F(t) - \beta F(t) \ln \left[ \frac{F(t)}{K} \right] \right\} dt + \sqrt{\sigma}F(t)dW(t). \quad (15)$$

The first term on the right hand side represents the growth due to the stressor, while the second represents the stress response. Note that mortality is treated here as dimensionless where the microscopic treatment would interpret  $F$  as cumulative probability of mortality, and the macroscopic equivalent would  
70 be the cumulative mortality.

To go from the microscopic to the macroscopic domain, we take the temporal average of (14), and use the property that the average of log-quantities is the logarithm of the median quantity, to obtain the familiar deterministic Gompertz differential equation in (1). We now see that by comparing (8a), (9) and the temporal average of (15) that

$$\sigma = 2\gamma_\infty \ln(Y_\infty), \quad (16)$$

---

<sup>1</sup>This perturbation model is also called an Ornstein–Uhlenbeck process



showing the relationship between the diffusion coefficient and the final conditions.

Thus, a more direct interpretation of the observations is that mortality was caused by a planetary perturbation, modeled as a random process, to which  
75 organisms gradually develop resistance at a geometric rate [21, 22]. Here, a geometric rate is an exponential rate in the log-transformed domain, which is the natural transformation for many processes in nature [23]. The log-normal distribution of the abundance of  $F$  can be obtained by solving the microscopic stochastic equation in 15 [24, 25]. In fact, Sitaram and Varma [26] showed  
80 using methods from theormodynamics that a variable undergoing Gompertz growth is log-normally distributed in its abundance (see also Gunasekaran and Pande [27]). This result is intuitively seen by noting that the solution to the perturbation model in the log-domain (14) is Gaussian in the variable  $Z(t)$ , thus suggesting a log-normal distribution of  $F(t)$ .

### 85 3. Unifying the SIR model and the Gompertz model

The remarkable observation that the log-transformed domain is the natural one merits closer study. First, juxtapose the logistic model with the Gompertz model,

$$\begin{aligned}\dot{F} &= \frac{d}{dt}F(t) = \beta F(1 - F) && \text{Logistic} \\ \frac{d}{dt} \ln(F(t)) &= -\beta \ln(F(t)) && \text{Gompertz}\end{aligned}\tag{17}$$

In the logistic model, we recognize the rightmost side of the logistic equation  
90 as the transmission term in an SIR model, but also as a linear interaction term between the two macroscopic states. Many studies do not consider microscopic effects at all, and the solution is obtained by solving the macroscopic (set of ODEs) [17]. This procedure is a mean field approximation with an implied average correlation between the variables. Thus, all dynamics are governed by  
95 macroscopic deterministic variables parametrized by a transmission rate.

Because the macroscopic logistic ODE solution never invokes the microscopic world, an imaginary microscopic solution could be modeled by splitting the system into  $N$  units,  $F(t) \rightarrow f_1(t), f_2(t)$ , etc, from which macroscopic growth would be obtained by taking the average over the individual units,

$$F(t) = \frac{1}{N} \sum_i^N f_i(t). \quad (18)$$

One could add network interaction necessitating a corresponding matrix version of (17),

$$\frac{df_i}{dt} = \beta(1 - f_i) \sum_j a_{ij} f_j \quad \forall i, \quad (19)$$

with a fixed correlation governed by the network's growth rate,  $b$ , and adjacency matrix,  $\{a_{i,j}\} = \mathbf{A} \in \mathbb{R}^{N \times N}$ , a binary matrix with ones where the  $i^{th}$  and  $j^{th}$  nodes are connected, and zeroes otherwise. Notice here that there is an implied causality going from the infected to susceptible, which will become relevant below. Furthermore, a linear correlation between variables is seen as the partial derivatives of the instantaneous growth rate with respect to pairs of microscopic variables,

$$\frac{\partial^2 \dot{F}}{\partial f_i \partial f_j} = -\frac{\beta}{N} a_{i,j}. \quad (20)$$

Still, no Gompertz curve will emerge at the onset of the growth process. Estrada and Bartesaghi [28] provide illuminating analysis on this topic.

In contrast, as shown in (14), the Gompertz model is implied by a multiplicative stochastic perturbation and thus correlated mortality growth, viz.

$$F(t) = \exp \left[ \frac{1}{N} \sum_i^N z_i(t) \right] = \left[ \prod_i^N f_i(t) \right]^{1/N}, \quad (21)$$

where the rightmost equality is due to the central limit theorem. Under this model, correlation between entities is present at all orders in the original domain<sup>2</sup>.

<sup>2</sup>It is illuminating to at this point compare with Gompertz' Law of Mortality,

$\frac{d}{dt} \ln(1 - F(t)) = -b$ , for  $t$  more than 25 years, which yields a naturally uncorrelated macro-

The remarkable observation that we see the Gompertz curve emerge at the macroscopic level implies that the system is indeed correlated, or coherent, presumably as a result of the simultaneous exposure to the same underlying stressor, but also due to the implied log-normal nature of the microscopic distributions [23]. We can now further appreciate Richard's parametrization as a transition from non-collaborative to collaborative growth as  $\theta \rightarrow 0$ . This feature of  $\theta$  was also obtained by Petroni et al. [15] by interpreting the  $\theta$ -logistic growth rate in (8) as non-linear resource availability dependent on the overall magnitude,  $Y(t)$ . Molski and Konarski [30] made a similar observation that Gompertzian growth is the coherent state in a quantum mechanical system with a time-dependent potential, an interpretation which sheds further light on the temporal nature of the postulated stress response. This quantum mechanical system has also been used to describe coherent energy states of diatomic molecules in space [31]. In the quantum mechanical world, *coherence* is a well-defined mathematical property first explored by Glauber [32] in the context of the electromagnetic field.

However, it is possible to reconcile the SIR model with the Gompertz curve from yet another argument. Inspired by the observation that in the linearized approximation there are only two coupled states, infected and susceptible, we augment the interaction term to higher orders. Then, we reverse the causality where the population of infected are now dependent of the population of the susceptible instead of the other way around as in (19). This latter change is a crucial change which is based on an environmental stressor rather than a communicable disease. Furthermore, we will for the sake of simplicity assume all nodes in the network have exactly one neighbor and that there exists a unique path between all nodes,

$$\sum_i a_{ij} = 1 \quad \forall j. \quad (22)$$

---

scopic curve  $1 - F(t) = \exp(-bt)$  [29]. In our context, the uncorrelated feature emerges since the force of mortality is not a function of the growth itself, as we see in the text, but rather of time.

If we let  $s_i = 1 - f_i$  be the probability of being susceptible, the augmented and causality-reversed SIR model becomes

$$\frac{df_i}{dt} = \beta f_i \sum_j a_{ij} (s_j + s_j^2/2 + \dots) - \alpha f_i \quad \forall i, \quad (23)$$

Now use the Taylor series  $x + x^2/2 + \dots = -\ln(1 - x)$ , viz.

$$\frac{df_i}{dt} = \beta f_i \sum_j a_{ij} \ln(1 - s_j) - \alpha = \beta f_i \sum_j a_{ij} \ln f_j - \alpha f_i \quad \forall i, \quad (24)$$

As we are interested in the aggregate behavior, we take averages in the log domain, exploit our setup where  $\mathbf{A}$  is a single mapping from one node to another, and simplify to the familiar Gompertz curve,

$$\frac{d}{dt} \ln \left[ \prod_i f_i \right]^{\frac{1}{N}} = -\beta \ln \left[ \prod_i f_i \right]^{\frac{1}{N}} - \alpha. \quad (25)$$

In this exposition, all the nodes in the network are communicating instantaneously. Lastly, if  $f_i \ll 1, \forall i$ , i.e. in the beginning of growth, the constant on  
120 the right hand side can be omitted. Another interpretation of  $\alpha \rightarrow 0$  could be that the limiting factor emerges purely from the growth rate without the need for a second constant parameter. One further simplification could be seen in equating the logarithm of the geometric mean with the logarithm of the median of the set of  $f_i$ .

#### 125 4. Conclusion

In conclusion, we have shown that Gompertz growth follows from infinite interactions between the susceptible and infected states, and the perceived pathogen travels at infinite speed throughout the population rejecting the possibility of a disease propagation stage through a perceived social network. In  
130 this vein, Richard's parameter  $\theta$  in his growth model paradigm can be related to the number of higher order interactions with the susceptible and the infected in an SIR model [14], where infinite interactions corresponds to  $\theta \rightarrow 0$ .

We further show that the observations can be explained by a model where the biological system is stressed by a ubiquitous and simultaneous stressor eliciting  
135 a corresponding stress response through which gradual return to pre-epidemic conditions are mediated. The stressor is modeled as a stochastic perturbation in the log-transformed domain of effects where correlation between people or microscopic entities are present at all orders. From this model, we draw parallels between the coherent behavior of the population's mortality evolution during an  
140 epidemic and the spatial coherence of quantum mechanical systems, borrowing the definition of coherence from the quantum world [30].

Thus, we see that we are at the intersection of a road: In one direction we find the non-collaborative growth models with parameterized linear interaction effects, and in the other direction we see a field of microscopic entities coherently  
145 sharing information much like quantum entangled particles. The emergence of coherent quantum phenomena at the macroscopic level suggests that no longer can the microscopic world claim a monopoly on quantum physics, especially as it relates to biology. One might be surprised to find that temporal evolution of human mortality during epidemics can behave like the spatial energy  
150 distribution of diatomic molecules.

## Supplement

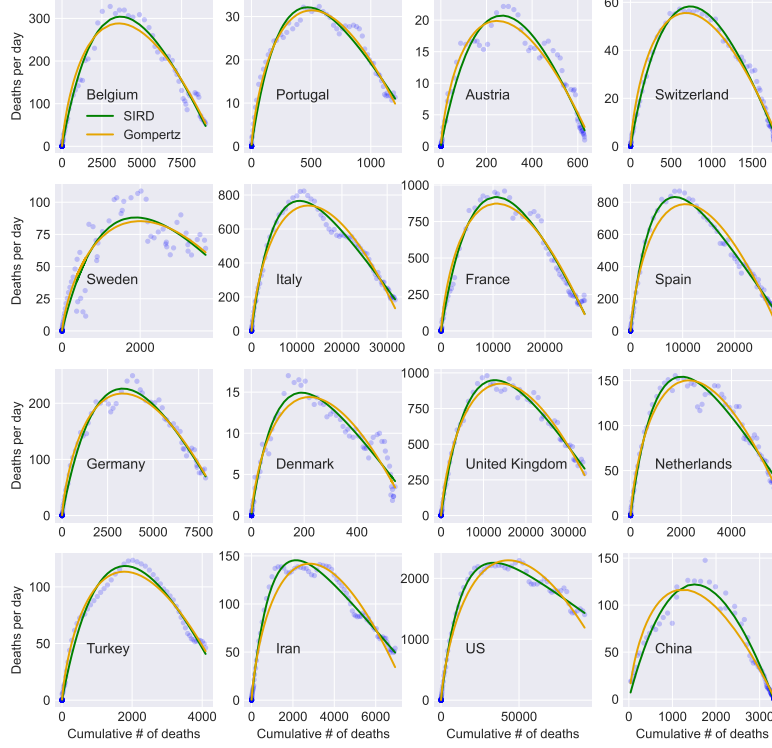


Figure 3: Cumulative diseased plotted against number of days after  $Y(t)/Y_{max} > 0.005$ , comparing an SIRD with a Gompertz model. Both models are fit using non-linear least squares according to equations (1) and (12) in the text. Fitting is done with Python-Scipy and a 6-day windowed average of deaths. Observations are taken from the Github repository compiled by the Center for Systems Science and Engineering (CSSE) at Johns Hopkins University, Baltimore, USA [19].

Table 1: Estimated values for the SIRD model fitted to various countries' observations normalized by the last observation,  $Y_{max}$ , as shown in Figure 2 using notation from 12. Note that due to normalization values will be different from Carletti et al. [5].

	$\eta \times 10$	$\xi$	$\kappa \times 10^2$
Belgium	1.0(1)	2.9(3)	9.3(1)
Portugal	0.55(4)	4.2(4)	4.5(4)
Austria	1.3(3)	2.3(4)	11(2)
Switzerland	1.24(1)	2.4(2)	11.0(7)
Sweden	0.5(2)	3(1)	3(2)
Italy	0.43(1)	5.6(2)	3.7(1)
France	0.88(7)	3.4(3)	8.1(6)
Spain	0.525(1)	6.2(2)	4.8(1)
Germany	0.78(8)	3.0(3)	6.5(7)
Denmark	0.50(4)	5.2(6)	4.2(4)
United Kingdom	0.54(2)	4.7(2)	4.3(2)
Netherlands	0.51(3)	5.0(4)	4.3(3)
Turkey	0.84(9)	2.8(3)	6.9(8)
Iran	0.322(7)	7.2(3)	2.51(9)
US	0.339(8)	7.0(3)	1.8(1)
China	3.8(9)	1.2(2)	26(4)

Table 2: Estimated values for the Gompertz model fitted to various countries' observations normalized by the last observation,  $Y_{max}$ , as shown in Figure 2 using notation from 1.

	$\nu \times 10$	$\beta \times 10^2$	$\tilde{Y} \times 10^2$
Belgium	2.74(1)	8.1(2)	3.6(3)
Portugal	2.242(6)	6.23(9)	3.1(1)
Austria	2.74(1)	8.1(2)	3.6(2)
Switzerland	2.740(7)	8.1(1)	3.6(2)
Sweden	1.73(3)	4.3(3)	2.6(4)
Italy	2.107(6)	5.88(9)	3.0(1)
France	2.752(1)	8.2(2)	3.6(2)
Spain	2.556(8)	7.5(1)	3.4(2)
Germany	2.335(7)	6.5(1)	3.2(1)
Denmark	2.32(1)	6.6(2)	3.2(3)
United Kingdom	2.333(6)	6.54(9)	3.2(1)
Netherlands	2.311(7)	6.5(1)	3.2(1)
Turkey	2.306(7)	6.4(1)	3.2(1)
Iran	1.862(7)	5.04(9)	2.7(1)
US	2.014(8)	5.3(1)	2.9(1)
China	3.155(8)	9.4(2)	3.6(2)

## References

- [1] T. Harko, F. S. Lobo, M. Mak, Exact analytical solutions of the susceptible-infected-recovered (sir) epidemic model and of the sir model with equal death and birth rates, Applied Mathematics and Computation 236 (2014) 184–194.
- [2] M. Kröger, R. Schlickeiser, Analytical solution of the sir-model for the temporal evolution of epidemics. part a: time-independent reproduction factor, Journal of Physics A: Mathematical and Theoretical 53 (2020) 505601.



- [3] R. Schlickeiser, M. Kröger, Analytical solution of the sir-model for the temporal evolution of epidemics: part b. semi-time case, *Journal of Physics A: Mathematical and Theoretical* 54 (2021) 175601.
- [4] K. Heng, C. L. Althaus, The approximately universal shapes of epidemic curves in the susceptible-exposed-infectious-recovered (seir) model, *Scientific Reports* 10 (2020) 1–6.
- [5] T. Carletti, D. Fanelli, F. Piazza, Covid-19: The unreasonable effectiveness of simple models, *Chaos, Solitons & Fractals: X* 5 (2020) 100034.
- [6] B. Gompertz, XXIV. on the nature of the function expressive of the law of human mortality, and on a new mode of determining the value of life contingencies. in a letter to francis baily, esq. f. r. s. &c, *Philosophical Transactions of the Royal Society of London* 115 (1825) 513–583.
- [7] A. D. Broido, A. Clauset, Scale-free networks are rare, *Nature communications* 10 (2019) 1–10.
- [8] A. Ohnishi, Y. Namekawa, T. Fukui, Universality in COVID-19 spread in view of the gompertz function, *Progress of Theoretical and Experimental Physics* 2020 (2020).
- [9] K. Rypdal, M. Rypdal, A parsimonious description and cross-country analysis of COVID-19 epidemic curves, *International Journal of Environmental Research and Public Health* 17 (2020) 6487.
- [10] M. Català, S. Alonso, E. Alvarez-Lacalle, D. López, P.-J. Cardona, C. Prats, Empirical model for short-time prediction of COVID-19 spreading, *PLOS Computational Biology* 16 (2020) e1008431.
- [11] T. Rodrigues, O. Helene, Monte carlo approach to model covid-19 deaths and infections using gompertz functions, *Physical Review Research* 2 (2020) 043381.

- [12] M. Levitt, A. Scaiewicz, F. Zonta, Predicting the trajectory of any COVID19 epidemic from the best straight line (2020).
- [13] M. Castro, S. Ares, J. A. Cuesta, S. Manrubia, The turning point and end of an expanding epidemic cannot be precisely forecast, Proceedings of the National Academy of Sciences 117 (2020) 26190–26196.
- [14] F. Richards, A flexible growth function for empirical use, Journal of experimental Botany 10 (1959) 290–301.
- [15] N. C. Petroni, S. De Martino, S. De Siena, Logistic and  $\theta$ -logistic models in population dynamics: General analysis and exact results, Journal of Physics A: Mathematical and Theoretical 53 (2020) 445005.
- [16] H. A. Herrmann, J.-M. Schwartz, Why covid-19 models should incorporate the network of social interactions, Physical Biology 17 (2020) 065008.
- [17] G. Vattay, Forecasting the outcome and estimating the epidemic model parameters from the fatality time series in covid-19 outbreaks, Physical Biology 17 (2020) 065002.
- [18] D. Smilkov, C. A. Hidalgo, L. Kocarev, Beyond network structure: How heterogeneous susceptibility modulates the spread of epidemics, Scientific reports 4 (2014) 1–7.
- [19] E. Dong, H. Du, L. Gardner, An interactive web-based dashboard to track covid-19 in real time, The Lancet infectious diseases 20 (2020) 533–534.
- [20] E. De Lauro, S. De Martino, S. De Siena, V. Giorno, Stochastic roots of growth phenomena, Physica A: Statistical Mechanics and its Applications 401 (2014) 207–213.
- [21] H. Boxenbaum, Hypotheses on mammalian aging, toxicity, and longevity hormesis: Explication by a generalized gompertz function, in: Biological Effects of Low Level Exposures to Chemicals and Radiation, CRC Press, 2017, pp. 1–39.

- [22] P. J. Neafsey, H. Boxenbaum, D. A. Ciraulo, D. J. Fournier, A gompertz  
215 age-specific mortality rate model of aging, hormesis, and toxicity: Fixed-  
dose studies, *Drug metabolism reviews* 19 (1988) 369–401.
- [23] C.-L. Zhang, F.-A. Popp, Log-normal distribution of physiological parameters and the coherence of biological systems, *Medical Hypotheses* 43 (1994) 11–16.
- [24] C. H. Skiadas, Exact solutions of stochastic differential equations: Gompertz, generalized logistic and revised exponential, *Methodology and Computing in Applied Probability* 12 (2010) 261–270.
- [25] N. C. Petroni, S. De Martino, S. De Siena, Gompertz and logistic stochastic dynamics: Advances in an ongoing quest, *arXiv preprint arXiv:2002.06409*  
225 (2020).
- [26] B. Sitaram, V. Varma, Statistical mechanics of the gompertz model of interacting species, *Journal of theoretical biology* 110 (1984) 253–256.
- [27] N. Gunasekaran, L. Pande, Log normal distribution for the intrinsic abundance of species from the gompertz model, *Journal of Theoretical Biology*  
230 98 (1982) 301–305.
- [28] E. Estrada, P. Bartesaghi, From networked sis model to the gompertz function, *Applied Mathematics and Computation* 419 (2022) 126882.
- [29] B. Shklovskii, A simple derivation of the gompertz law for human mortality, *Theory in Biosciences* 123 (2005) 431–433.
- [30] M. Molski, J. Konarski, Coherent states of gompertzian growth, *Physical review E* 68 (2003) 021916.  
235
- [31] P. M. Morse, Diatomic molecules according to the wave mechanics. ii. vibrational levels, *Physical review* 34 (1929) 57.
- [32] R. J. Glauber, Coherent and incoherent states of the radiation field, *Physical Review* 131 (1963) 2766.  
240